Journal of Air Pollution and Health (Winter 2023); 8(1): 87-102

Original Article

Available online at http://japh.tums.ac.ir

A study to access and estimation of air pollution using a multivariate statistical model in Chennai, India

Yuvaraj Ramachandran Muthulakshmi[1,*], *Sakthivel Mathivanan*[1], *Marangattu Raghavan Sindhumol*[2]

[1] Department of Geography, University of Madras, Chennai, Tamil Nadu, India
[2] Department of Statistics, University of Madras, Chennai, Tamil Nadu, India

ARTICLE INFORMATION

Article Chronology:
Received 05 December 2022
Revised 30 January 2023
Accepted 20 February 2023
Published 29 March 2023

Keywords:
Air pollution; Particulate matter; Particulate matters less than 2.5 µm ($PM_{2.5}$); Particulate matters less than 10 µm (PM_{10}); Multivariate statistical model

CORRESPONDING AUTHOR:

yuvaraj1023@gmail.com
Tel: (044) 24866001
Fax: (044) 24866001

ABSTRACT

Introduction: Rapid urbanization and industrial growth are the primary causes of deteriorating urban air quality in developing countries, including India. Vehicular emission is a significant cause of the degradation of air quality. It includes Air Pollution like carbon monoxide, hydrocarbons, oxides of nitrogen, oxides of sulfur, Suspended Particulate Matter (SPM), respiratory Particulate Matters ($PM_{2.5}$ and PM_{10}), and lead.

Materials and methods: The study has considered land use,land cover, land surface temperature, vegetation, literacy rate, vehicle population, population density, and households, finding the responsible causes of air pollutionfor the analysis. Supervised classification using ArcGIS for extracting land use and land cover, Least Slack Time (LST) algorithms have used to extract land surface temperature, spatial interpolation methods like Inverse Distance Weighting (IDW) using ArcGIS for identifying the spatial distribution of Literacy rate, vehicle population, population density and households and finally the multivariate statistical model applied to identify the major responsible factor for air pollution using SPSS.

Results: The study reveals that the particulate matter is below the standard value prescribed by the central pollution control board. The Highest air pollution is primarily responsible for vehicle population and industries. Wednesday and Thursday are the maximum pollution in Chennai, whereas it was recorded as very low on Sunday as compared to other days.

Conclusion: Regression shows that the vehicle population is responsible for air pollution, followed by the population.

Introduction

Vehicle exhaust, on-road re-suspended dust owing to vehicles, industrial fumes, construction dust, waste burning, residential cooking and heating, and some seasonal sources such as agricultural field residue burning and dust are all contributing to urban air pollution [1]. An increase in urban and industrial areas significantly contributes to deteriorating urban air quality, particularly in developing countries like India. Vehicular emission is a significant cause of the degradation of air quality. It

Please cite this article as: Muthulakshmi YR, Mathivanan S, Sindhumol MR. A study to access and estimation of air pollution using a multivariate statistical model in Chennai, India. Journal of Air Pollution and Health. 2023;8(1): 87-102.

includes Air Pollutants (APs) like Particulate Matter (PM), Oxides of Nitrogen, carbon monoxide, Oxides of Sulfur, hydrocarbons, Suspended Particulate Matter (SPM), and lead [2]. Most remarkably, the re-suspension of road dust due to rubber wheels and brake wear also generates large amounts of PM_{10} [3]. An insufficient change in the physical, chemical, or biological characteristics of air that impedes life and may cause health problems is called air pollution [4]. Air Pollution, in particular, irritates the eyes, lungs, nose, and throat. It also causes respiratory problems and aggravates pre-existing conditions like asthma and emphysema. The risk of cardiovascular disease escalates when humans are constantly exposed to air pollution. The harmful health effects of air contamination depend on the pollutant source, the source's potency, and the potentially exposed individual's behavior [5]. Air pollution has been projected to cause over 4 million premature deaths each year, and levels of air pollution are still rising in certain places [6].

Ambient airborne Particulate Matter (PM), which occurs in various sizes and chemical and biological components, is a major scientific and policy problem [7]. PM is responsible for most of the illness burden related to air pollutants, with more than half relating to ambient inhalation exposures. Among the significant risk factors threatening human health globally concerning its disease burden, PM has recently been ranked fifth and thus first among environmental risks. The current levels of city air pollution need to be evaluated and managed to givethe residents a healthy urban air environment.Numerous studies on outdoor land plants or vegetation as interventions capable of protecting our health from ambient air pollution at various scales have been inspired by rapid urbanization and increased awareness of the effects of the natural environment on our health [8, 9]. In India, air pollution is the third leading cause of death among health risks, and as a result, life expectancy has decreased by 2.6 years. As a result, it has become increasingly important to control pollution and effectively educate people affecting air quality to maintain a healthy standard. Temperature is another parameter that will increase air pollution with temperature increases. Extreme heat and stagnant air during a heat wave increase particulate pollutants. Demographic factors such as population density, household size, and literacy rate also affect the air pollution standard [10]. Thus, investigating the assessment of air pollution exposure and its influencing factors will benefit community health and well-being. This information will inevitably improve personal responses to pollutants or a specific harmful agent [11]. Theseair pollutants of $PM_{2.5}$ and PM_{10} have been used in conjunction with GIS to analyze and visualize spatial and temporal impacts of air pollution in Chennai [12]. Spatial interpolation methods like Inverse Distance Weighting (IDW) have been extensively used to foresee the concentration of air pollution [13-15].

Study area

The state executive and legislative headquarters are principally housed in the Secretariat Buildings on the Fort St George complex in Chennai, which serves as the capital of Tamil Nadu. The Chennai Metropolitan Development Authority (CMDA) is the central agency in charge of planning and development in the Chennai Metropolitan Area, which spans 1,189 km^2 (459 sq mi) and includes parts of the Tiruvallur and Kanchipuram districts. Although it is the smallest of the state's districts, it has the highest population density. The city has an area of 426 km^2. Chennai is the 4th most populated city, the 6th most densely inhabited city in India, and the 31st biggest urban in the world.

The area of the city possesses the rank of 27 out of 640 cities in India. It is the 'Gateway to South India' and is well-connected globally. Chennai is northeast of Tamil Nadu, on the east shore, next to the Bay of Bengal. It lies between the 12°50'43.615"N and 13°13'49.196"N latitudes and 80°8'37.79"E and 80°19'52.827"E longitude (Fig. 1). It extends 25.6 km along the bay coast, from Thiruvanmiyur in the south to Thiruvottiyur in the north. It runs inwards in a robust semicircular shape. It limits the east with the Bay of Bengal and the other three sides with the districts of Kanchipuram and Thiruvallur (Fig. 1).

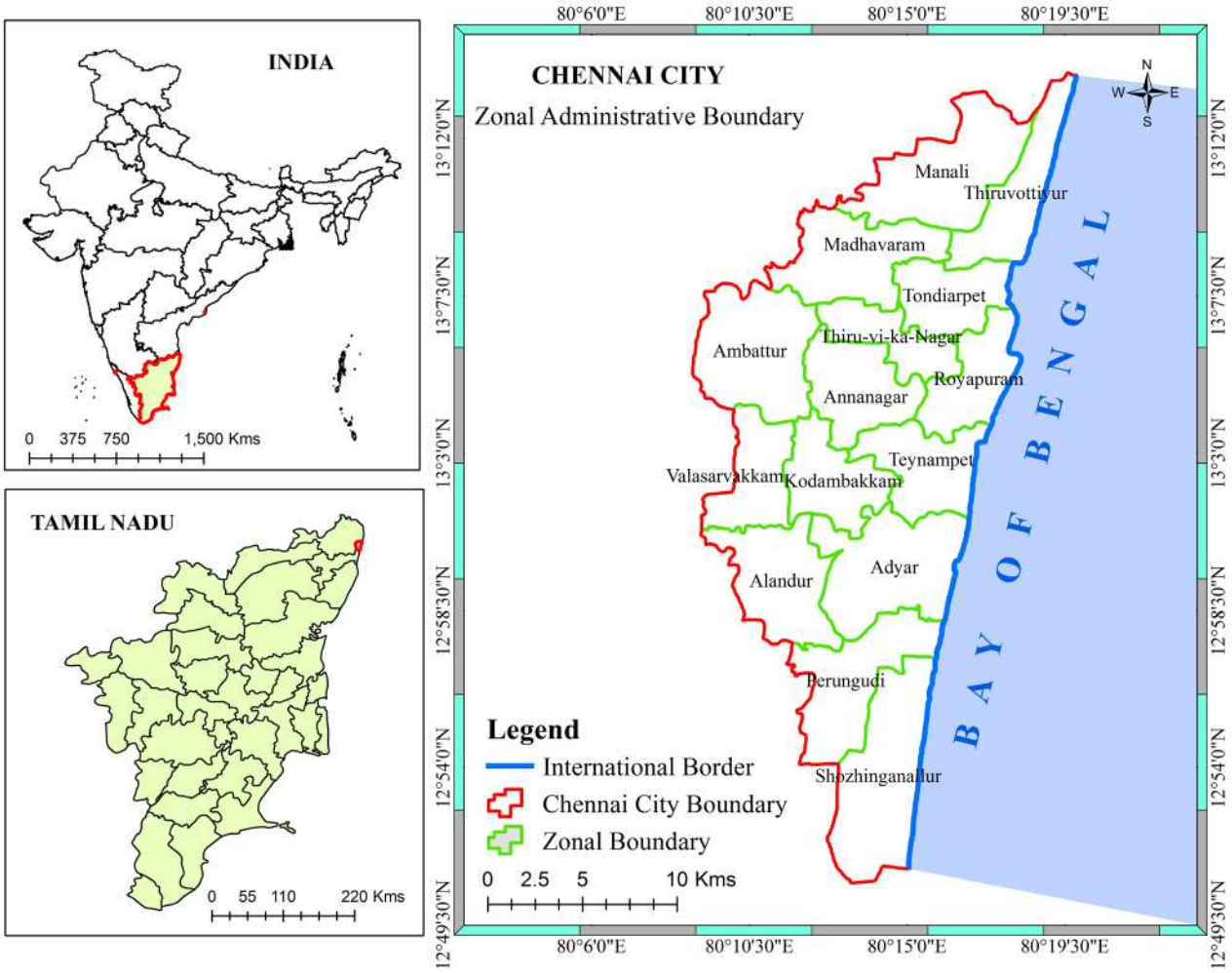

Fig. 1. Study area–Chennai city

Materials and methods

For finding the Land Surface Temperature (LST) of the study region, Landsat 8 Operational Land Imagers (OLI) and Thermal Infrared Sensor (TIRS) images with 143 paths and 51 row has used. These images have been downloaded from USGS (United States Geological Survey), which contains 11 bands with different wavelengths. These satellite images have been utilized to estimate the LST and vegetation. Particulate Matter ($PM_{2.5}$ and PM_{10}) air pollution data has been gathered from the Central Pollution Control Board (CPCB) for 2021. Demographic data like population, literacy rate, Household, and population density from the census of India, Chennai for the year 2011.

The satellite photos were preprocessed by extracting images based on the research region using the ArcGIS 10.2 extract by mask tool. The research region and accompanying satellite pictures are obtained after preprocessing for data analysis. Only bands 10, 4, and 5 are used to calculate the Land Surface Temperature in this study (LST). Thermal Infrared Sensor (TIRS) band 10 has a wavelength of 10.60 to 11.19, red band 4 has a wavelength of 0.64 to 0.67, and Near Infrared (NIR) band 5 has a wavelength of 0.85 to 0.88. The land surface temperature of the research region was determined using the following algorithm.

Calculation of top of atmospheric (TOA)

The introductory course of action for retrieving land surface temperature is estimating the spectral radiance of TOA.

$$\text{TOA (L)} = M_L * Q_{Cal} + A_L - O_i \quad (1)$$

Where ML signifies the precise band's multiplicative rescaling factor, Q_{cal} signifies the Quantized and calibrated standard product pixel values (DN), AL signifiesthe precise band's Additive rescaling factor, and O_i is the band correction from Table 1 [16].

Calculation of Brightness Temperature (TB)

The next step is transforming spectral reflectivity to TB using metadata's constant values. The reflectance was converted to brightness temperature using the equation below.

$$TTB = \frac{K_2}{In\left[\left(\frac{K_1}{L}\right)+1\right]} - 273.15 \quad (2)$$

Where K_1 and K_2 signify the specific band's thermal conversion constants, L signifies the Top of the atmosphere. In order to achieve the outcome value in Celsius, the radiant temperature is adjusted by summing the absolute zero (-273.15 0 C).

Calculation of land surface emissivity (LSE)

Since the LSE is a proportionality factor that scales blackbody radiance (Planck's law) to forecast emitted radiance, and it is the competence of transporting thermal energy across the surface into the atmosphere, it is necessary to know the LSE factor in order to compute the LST [17]. As a result, the emissivity is computed using the equation below.

$$\varepsilon = \varepsilon_v P_v + \varepsilon_s(1 - P_v) + d\varepsilon \quad (3)$$

Where $\varepsilon_v$signifies the emissivity of the vegetative of the region and $\varepsilon_s$signifies the emissivity of the soil, $P_v$signifies the proportion of vegetation of the region [18]. Following a research., the ultimate emissivity for the Landsat 8 image is specified by the equation given below [19].

$$\varepsilon = 0.004\ Pv + 0.989, \quad (4)$$

Where 0.004 signifies the standard deviation of 49 soil spectra, 0.989 signifies the average emissivity of the region's soil (0.97) and the region's vegetation's emissivity (0.99).

Table 1. Metadata for the Landsat 8

Constant	Factor	Band	Value
M_L	Band's rescaling feature	10	0.000342
A_L	Band's rescaling feature	10	0.1
K_1	Thermal constant value	10	1321.08
K_2	Thermal constant value	10	777.89
O_i	Correction	10	0.29

Calculation of vegetation and its share

The share of vegetation of a region (P_v) is estimated based on the following given equation [20].

$$P_v = \left(\frac{NDVI - NDVI_{min}}{NDVI_{max} - NDVI_{min}}\right)^2 \quad (5)$$

With the use of Landsat visible (band 4) and NIR (band 5) data, the following equation is used to determine the Normalized Difference Vegetation Index (NDVI). When identifying the LST, the amount of vegetation present is crucial [21].

$$NDVI = \frac{NIR - Red}{NIR + Red} \quad (6)$$

Calculation of land surface temperature (LST)

The concludingprocedure for calculating the LST is based on the following equation [22].

$$LST = \frac{TB}{\left\{1 + \left[\frac{\lambda TB}{\rho}\right] In\ \varepsilon_\lambda\right\}} ℃ \quad (7)$$

Where λ signifies the wavelength of emitted radiance by Landsat 8, which is 10.8 (given by NASA), ε_λ signifies the emissivity of the land surface, ρ is given by the equation given below,

$$\rho = h\frac{c}{\sigma} = 14388\ \mu m\ K \quad (8)$$

Where h signifies Planck's constant (6.626 X10^{-34} Js) , σ signifies the Boltzmann constant (1.38 x 10^{-23} J/K), and c signifies the velocity of light (2.988 x 10^8 m/s) [20]. The land Surface Temperature for the study region has been done for March 2021.

Statistical model

SPSS was used to develop a statistical model using multiple linear regression (statistical package for the social science).

$$Y = \alpha + \beta_1 x_1 + \beta_2 x_2 + \beta_3 x_3 \quad (9)$$

Where Y signifies the dependent variable, α signifies the intercept, $\beta_{1,2,3}$……. are regression coefficients of the independent variables, $x_{1,\ 2,\ 3}$ ….. are independent variables which would be the predictor of the dependent variable.

A supervised signature extraction with the maximum likelihood algorithm was employed to classify the digital Land use Land cover mapping for 2021. An extensive field survey was conducted throughout the research area utilizing Global Positioning System (GPS) equipment before the preprocessing and classification of satellite pictures began. This survey was conducted to acquire accurate locational point data for each Land Use Land Cover class in the categorization method, establish training sites, and generate signatures. The NRSC (National

Remote Sensing Centre) categorization system was used to classify land use/land cover (agriculture, built-up, wetlands, and wasteland). Using the picture interpretation element (such as tone, texture, shape, pattern, and association) and Arc-GIS software, the Indian Remote Sensing Satellite (IRS) data were visually and digitally interpreted. Before the theme maps were finalized, adequate field checks were performed.

Results and discussion

Distribution of particulate matter

Spatio-temporal distribution of air pollutant $PM_{2.5}$ for Chennai city has shown in Figure 2. Spatially northern parts of Chennai have high pollution of $PM_{2.5}$ as compared to the southern part. Wednesday and Thursday show the maximum $PM_{2.5}$, and Sunday records are low as compared to other days. Manali village has a high average of $PM_{2.5}$, followed by Kodungiyur and Arumbakkam, whereas Manali has recorded a low, followed by Perugudi shown in Figure 3. Spatio-temporal distribution of air pollutant PM_{10} for Chennai city has shown in Figure 3. Spatially northern parts of Chennai have high pollution of PM_{10} as compared to the southern part. Wednesday and Thursday show the maximum PM_{10}, and Sunday records are low as compared to other days. Manali village has a high average of PM_{10}, followed by Manali and Arumbakkam, whereas Velachery has a recorded low, followed by Perugudi and Royapuram, showed in Figure 5. Particulate matter ($PM_{2.5}$ and PM_{10}) is below the standard value prescribed by the Central pollution control board given in Table 2. Similarly, some resaearchers have reported that $PM_{2.5}$ has increased to 10 units from the normal period to the vacation period, whereas PM_{10} has increased to 22 units during the same period in Latin America Megacity [23].

Population and density

Chennai is one of the largest cities in South India, with a population of 72,53,531. The city's population increased from 17,49,000 (1966) to 72,53,531 (2011), and its area increased from 128.83 km^2 in 1961 to 426 km^2 in 2011, with the population density increasing from 128.83 to 17027 during the same period. Being an important commercial centre of the state, Chennai's population has experienced rapid population growth.

Table 2. National Ambient Air Quality Standards

S. No	Pollutant	Concentration in air ($\mu g/m^3$)
1	PM_{10}	100
2	$PM_{2.5}$	60

Source: CPCB, 2019

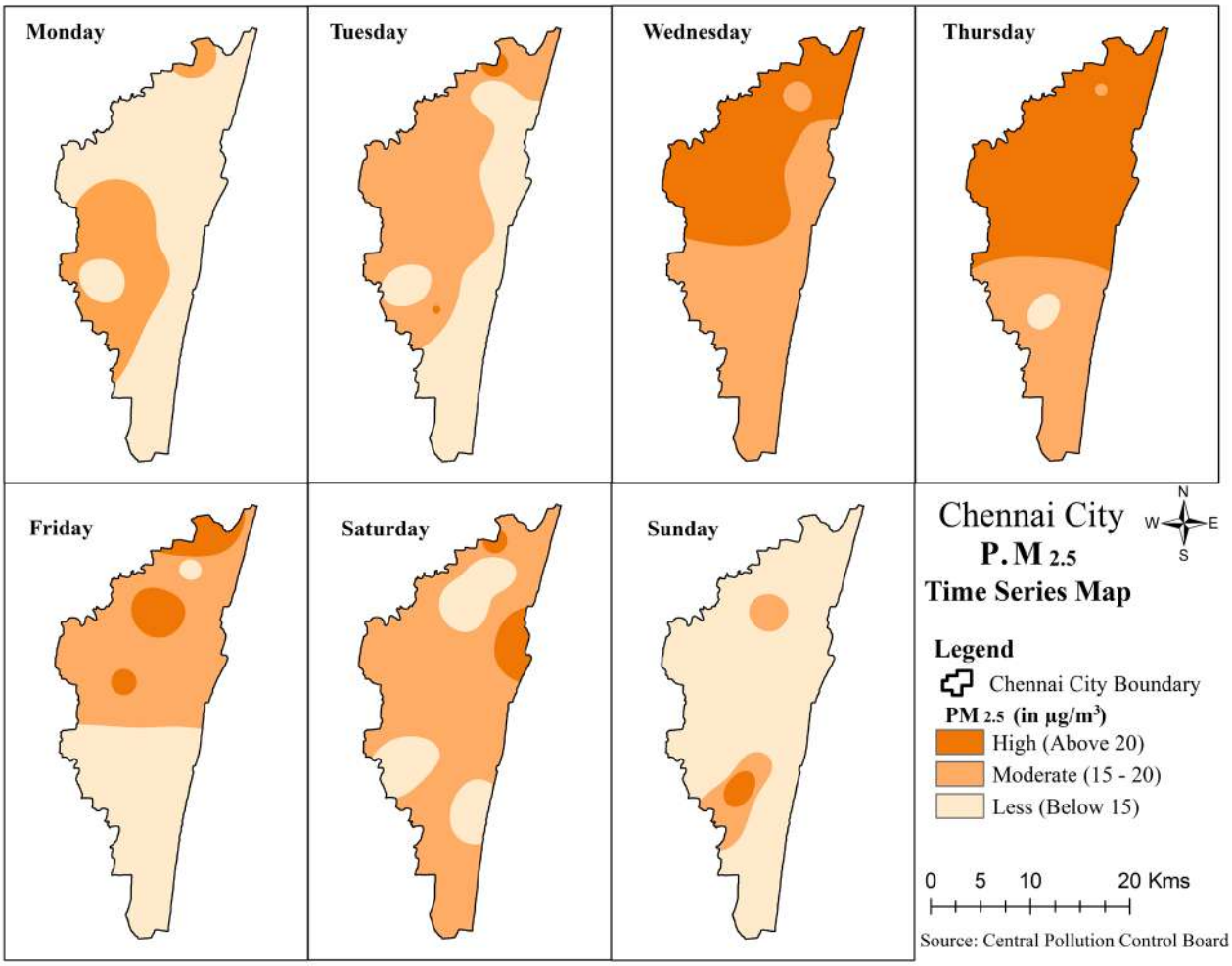

Fig. 2. Spatio-temporal distribution of $PM_{2.5}$- 2021

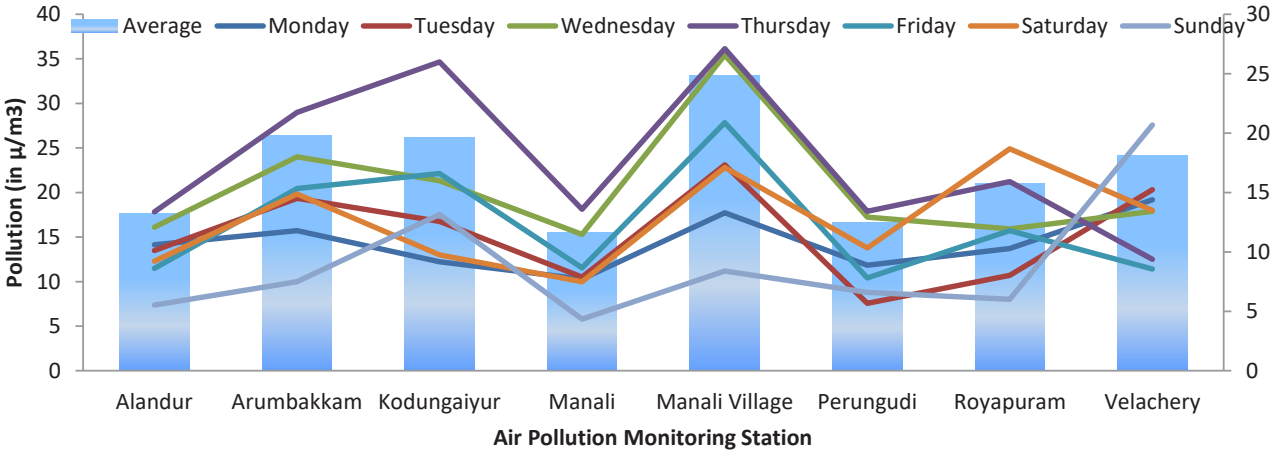

Fig. 3. Distribution of $PM_{2.5}$ – 2021

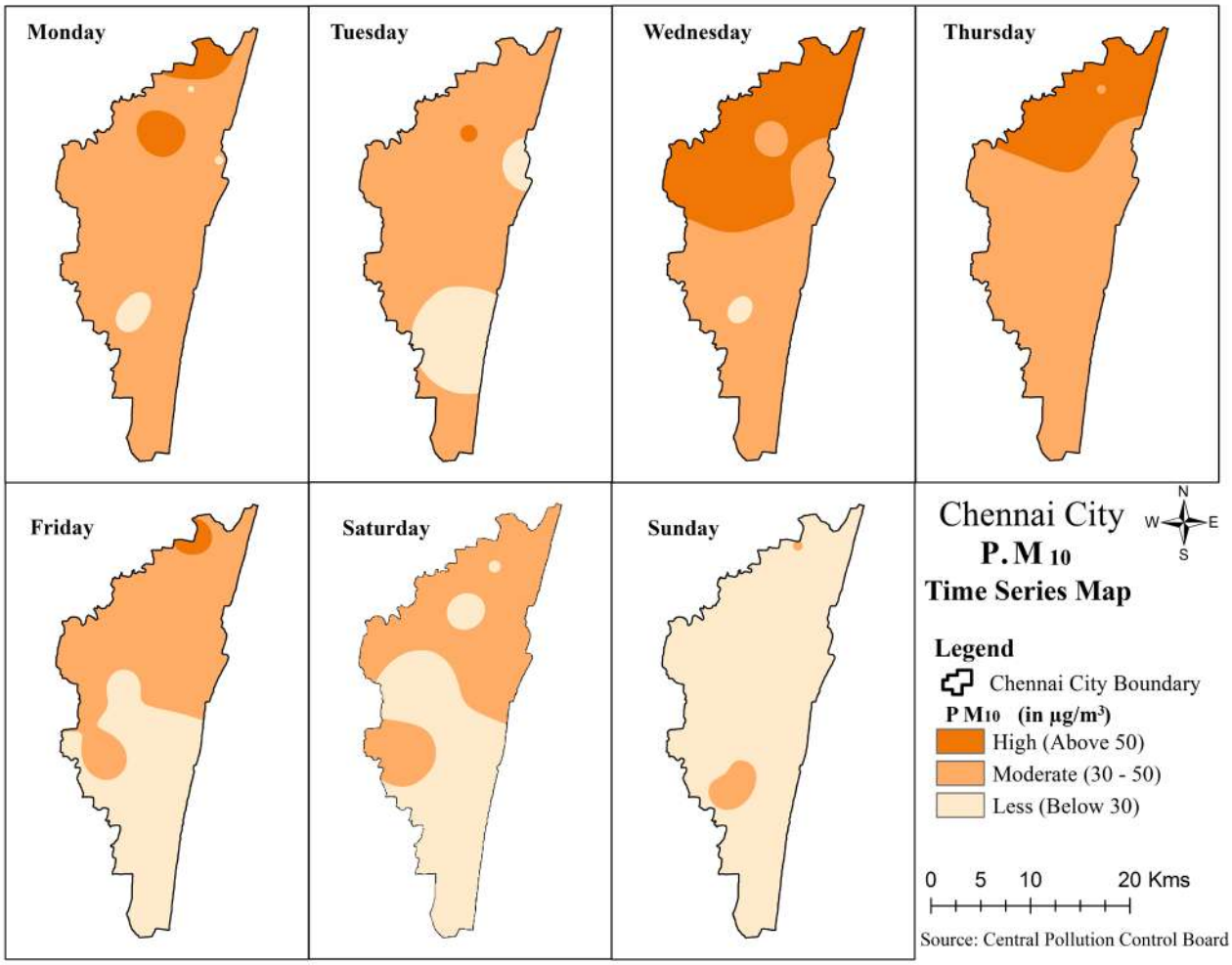

Fig. 4. Spatial and Temporal Distribution of PM_{10} - 2021

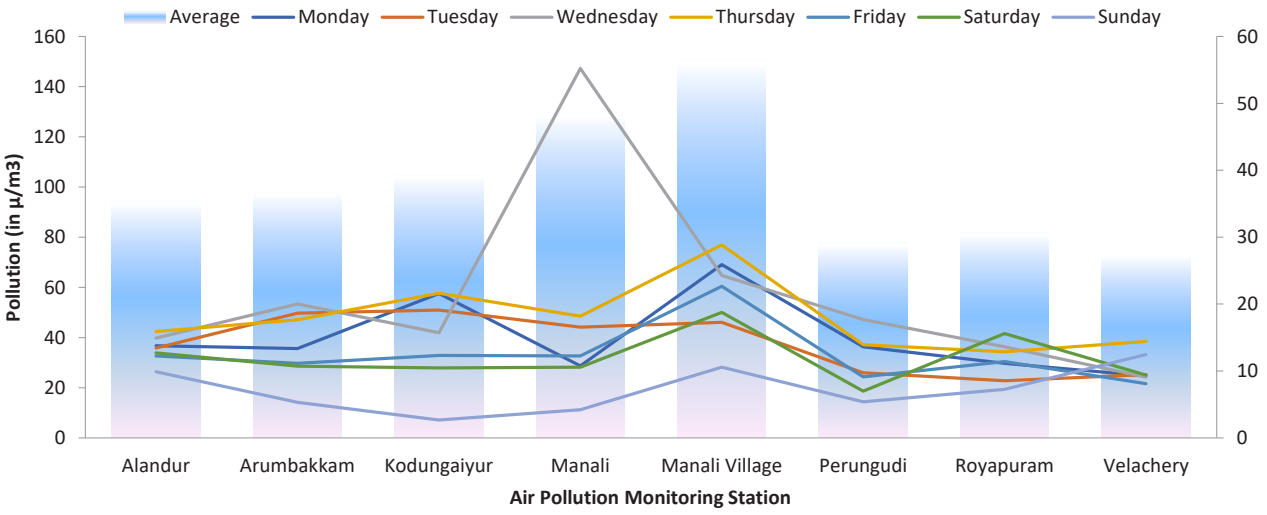

Fig. 5. Distribution of PM_{10} – 2021

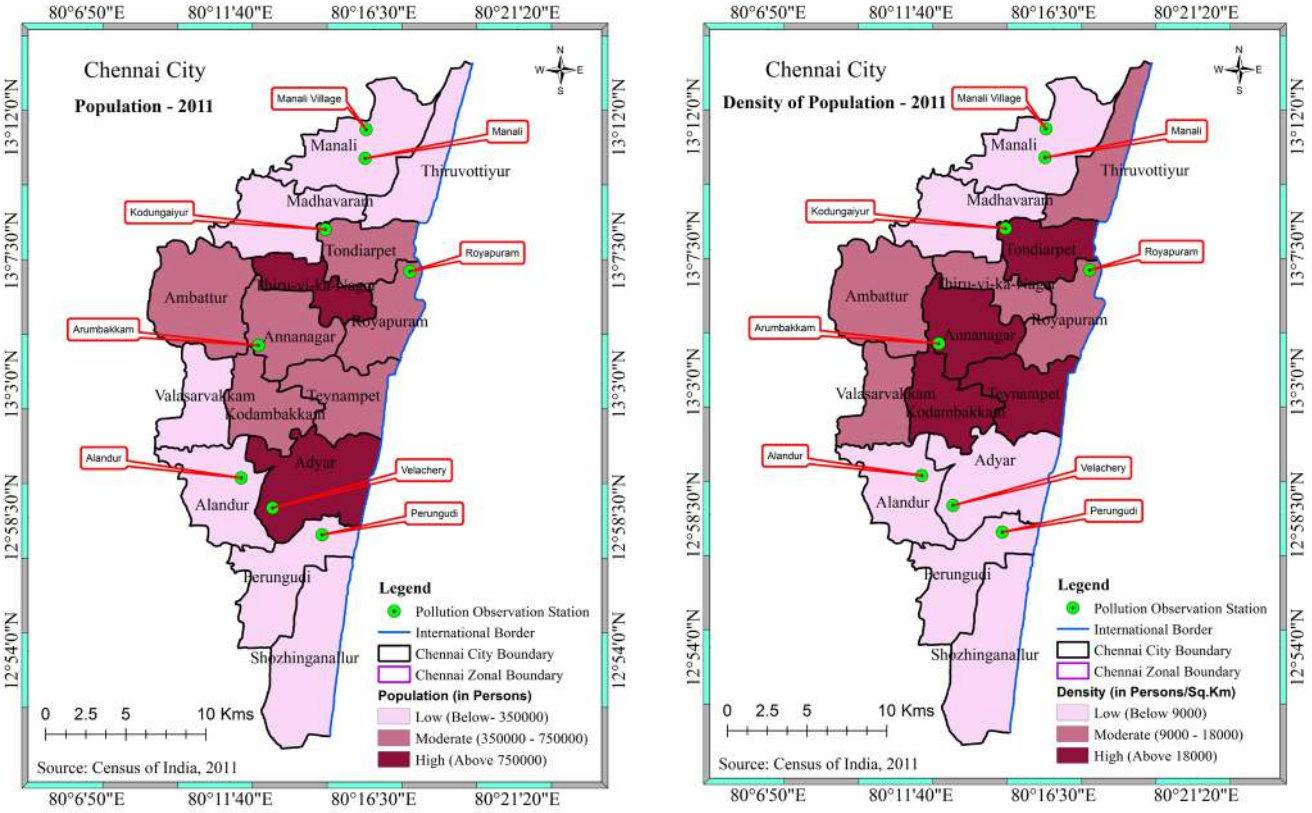

Fig. 6. Population and density of population

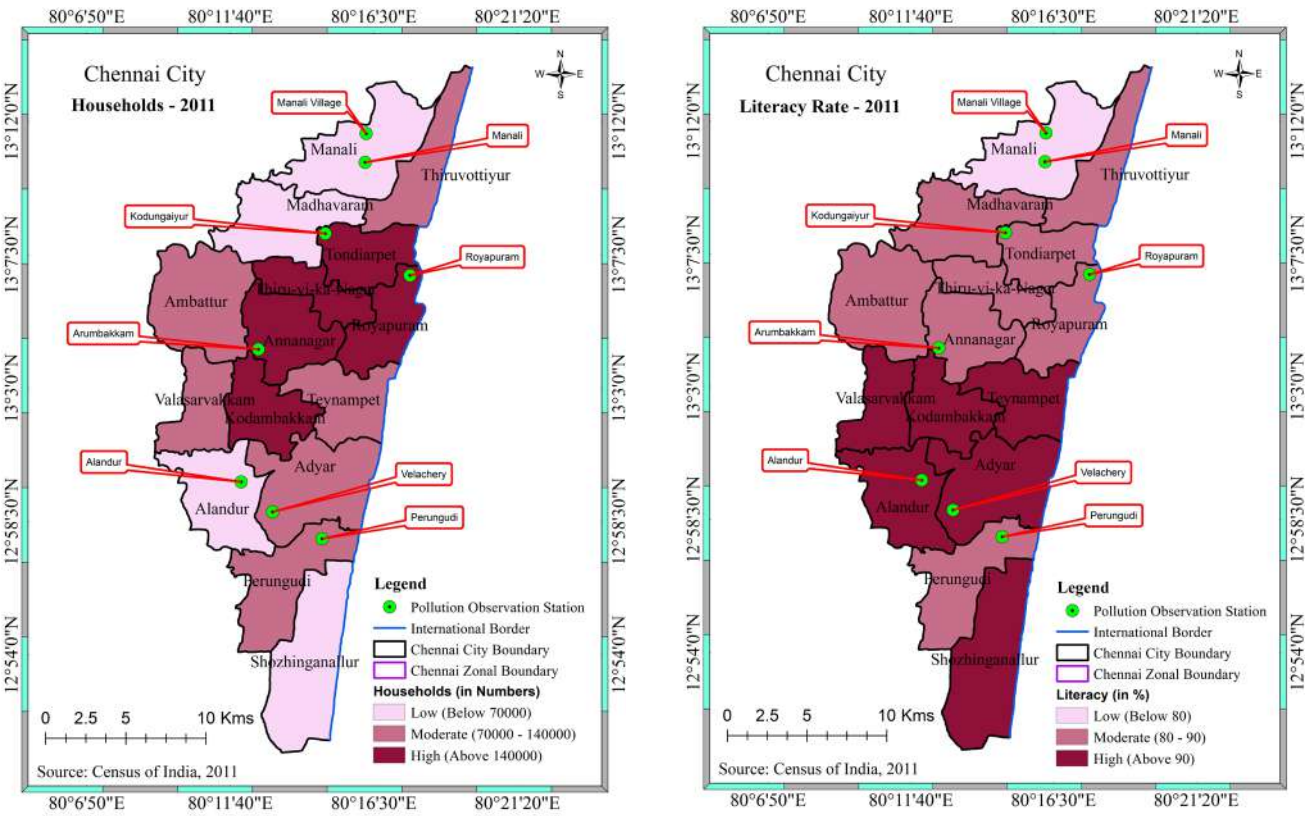

Fig. 7. Household and literacy rate

Chennai has become an important destination for trade and tourism in recent years. Due to its economic viability and available infrastructure, the city was referred to with enormous potential for industrial growth. According to the 2011 Census for Chennai, the population density is 26,553 people per km^2. Around 175 km^2 of the area is urban, though no rural area exists. Moreover, Anna Nagar, Tondairpet, Kodambakkam, and Teynampet zones had very high population density and female population density compared to Chennai city zones (Fig. 6). Researchers in a study reported that the population in urban area significantly impacts the air quality in China [24].

Households

According to the 2011 census, the Chennai district has 1.1 million families, with 51% in rented houses. Household is also very high in Thiru vi ka Nagar zone when comparing other zones in Chennai city followed by Royapuram, Kodambakkam and anna nagar zone. The lowest household population is in Sholinganallur and Manali zone, in the south and north extreme, respectively.

Literacy Rate

The mean literacy ratio in 2001 was 85.33 %, and 90.33 % in 2011. It is expressed much higher than the national mean of 79.5 %. Out of 3,776,276 literates, 1,968,079 were males (93.7%), while 1,808,197 were females (86.64%) in the Chennai district. Adyar, Kodambakkam, and Teynampet zones had very high female literacy rates when comparing other zones in Chennai city (Fig. 7).

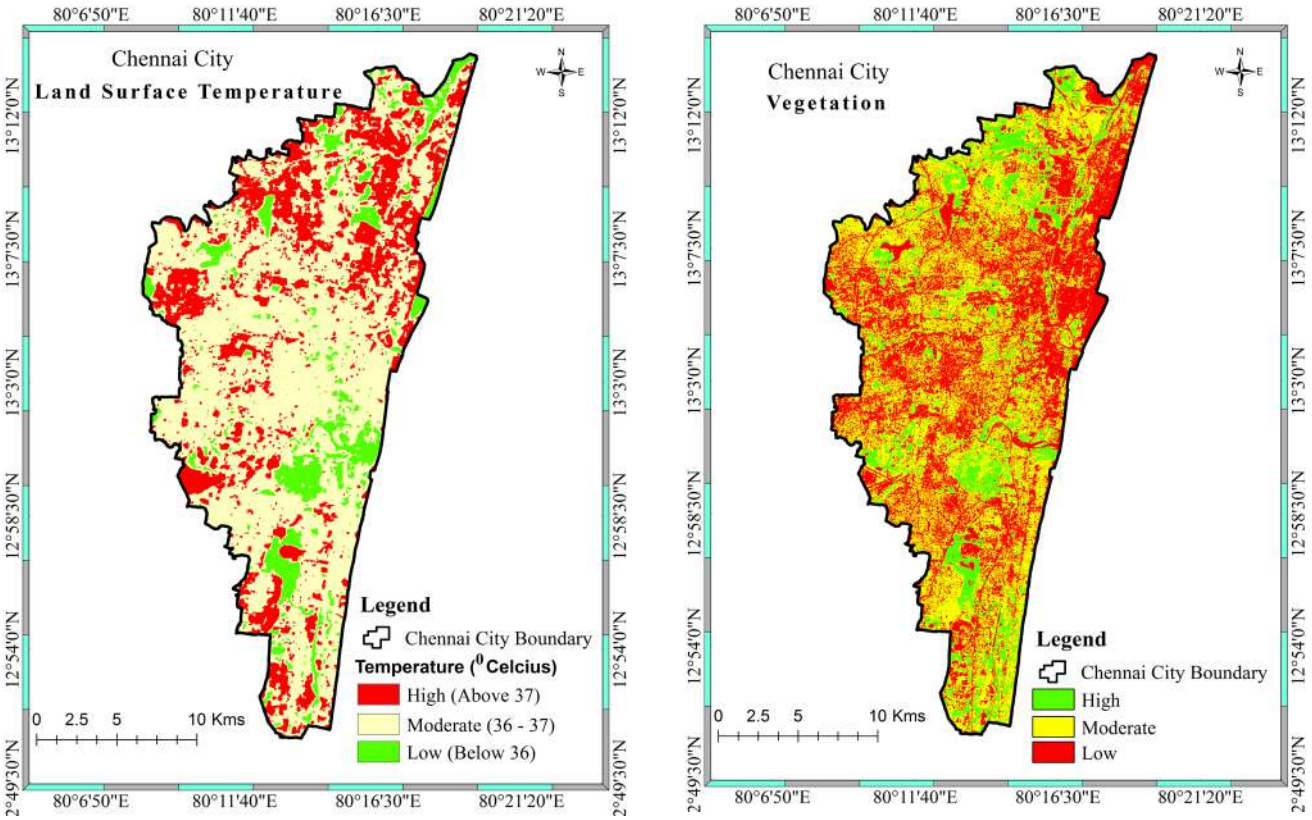

Fig. 8. Land surface temperature and vegetation - 2021

Land surface temperature (LST)

The land surface temperature has been identified using band 4, band 5 and band 10 of the Landsat image, a satellite image from the United State Geological Survey (USGS). Chennai city is located in a tropical region that receives maximum solar radiation, which triggers the land surface temperature, which will be regulated due to various reasons such as vegetation and water body. The Chennai region has been classified into three categories based on high, moderate and low land surface temperature. High LST is a region above 370C; moderate LST regions are between 360 C to 370 C; low LST is a region below 360 C. High LST occupies 108 sq. km (23%), moderate LST occupies 275 km^2 (24 %). Low LST occupies 44 sq. km (10 %) (Fig. 8). Similarly, some researchers have reported that the temperature in urban area significantly impacts the air quality in China [24].

Vegetation

The NDVI is a dimensionless index that reflects the variation in vegetation cover's visible and near-infrared reflectance and can be used to assess the density of green on a piece of Land. High vegetation in Chennai city occupies 39 km^2, 13% of the total area. Moderate vegetation occupies 195 km^2, which is 45% of the total geographical area of Chennai city. Low vegetation occupies 173 km^2, 40% of the total geographical area. Vegetation is maximum in the northern part and southern parts of Chennai (Fig. 8). Researchers has reported that the vegetation in the urban areasignificantly impacts the air quality in China [24].

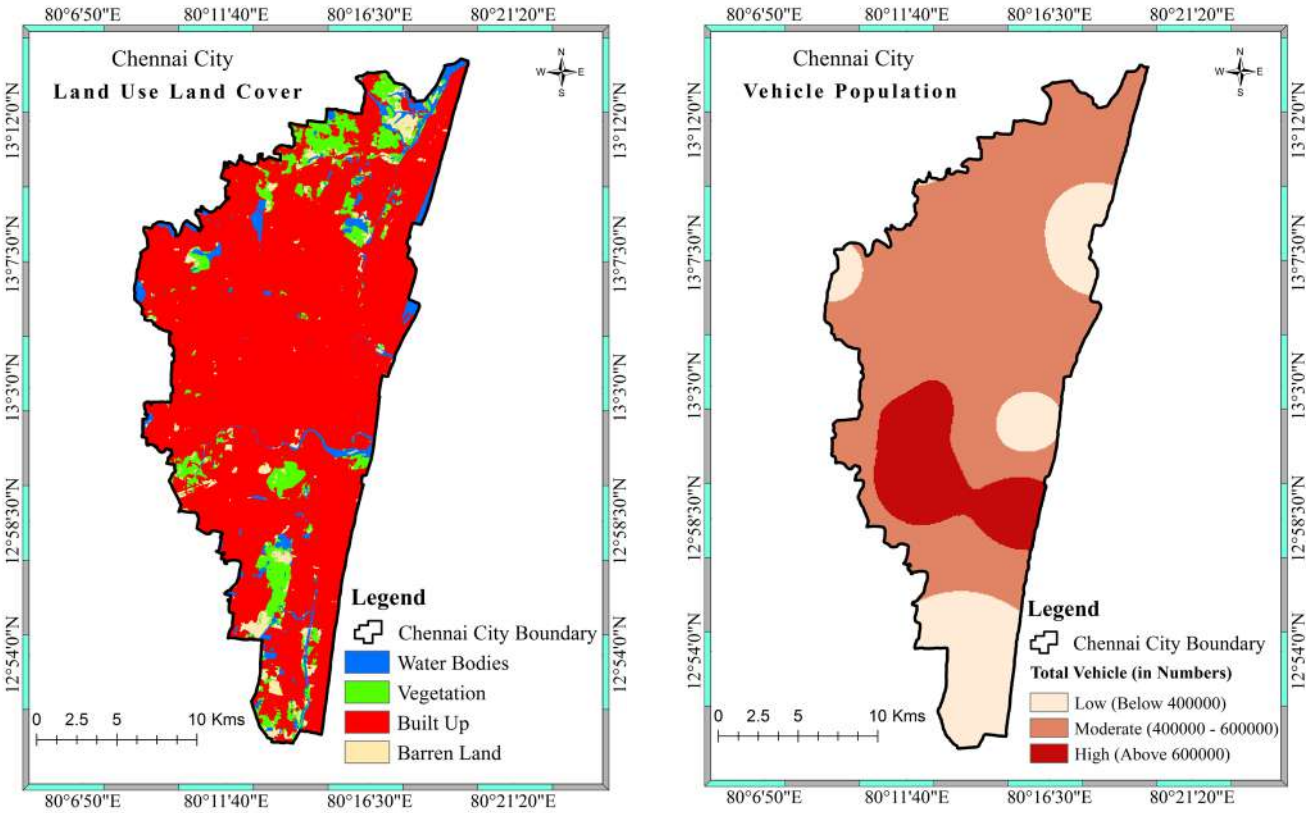

Fig. 9. Land use land cover and vehicle population-2021

Land use land cover (LULC)

LULC for Chennai has performed for 2021 with type 1 classification based on National Remote Sensing Corporation (NRSC). LULC classification of vegetation, built-up, water body and Barren Land has been demarcated. Vegetation features cover 34 km^2, which occupies 8% of the total area; built features are covered the maximum area of Chennai city with 357 sq. km, which is 83% of the total Chennai area. The water body covers 21 km^2 with 5% of the total area. Finally, the Barren land feature covers 14 km^2, which is 3.5% of the total area of Chennai city. Chennai city has three rivers: the Kosasthalaiyar river, with a total length of 136 km; the Coum river, with a total length of 64 km; and the Adyar river, which runs 42 km (Fig. 9).Similarly, researchers have reported that the buildup area has significantly impacted the air quality in China [24].

Vehicle population

Overall, Chennai the vehicle population is moderate level. In the Adyar, Alandur, Kodambakkam, and Valassaravakkam regions, the vehicle population is high, whereas, in Shozhinganallur and Tondiarpet, the vehicle population is less shown in Fig. 9.

Prediction model

The model performed based on multiple regression shows that the model predicting the responsible factor for $PM_{2.5}$ is significant with a correlation of 0.769, which is high. It reveals that the dependent variable is 76.9% predicting the air pollution for $PM_{2.5}$. Similarly, the model predicting the responsible factor for PM_{10} is significant, with a correlation of 0.854, which is high. It reveals that the dependent variable is 85.4% predicting the air pollution for PM_{10} shown in Table 3. Researchers has studied that automobile exhaust gas is discharged into the air, causing severe air pollution in Beijing, China [25].

The parameters such as LST and Vegetation has not significant in both pollutants ($PM_{2.5}$ and PM_{10}), revealing that neither LST nor Vegetation is not determining the air pollution in Chennai city. Literacy rate and Land use, land cover, and vegetation show negative values on both pollutants, which means air pollution and literacy rate, LULC and vegetation are inversely proportional. In contrast, households, population density, and vehicle population are directly proportional to air pollution, particularly $PM_{2.5}$ and PM_{10}. Vehicle population has more responsible for particulate matter, followed by density, households and population shown in Table 4.

Table 3. Model summary

Model	R	R^2	Sig. F Change
$PM_{2.5}$	.769[a]	.448	.000
PM_{10}	.854[a]	.729	.000

Table 4. Coefficient of regression

Parameters	$PM_{2.5}$		PM_{10}	
	B	Sig.	B	Sig.
(Constant)	18.237	0.000	55.476	0.000
Households	1.128	0.000	5.074	0.000
Densityof Population	1.573	0.000	3.910	0.000
Literacy Rate	-1.434	0.000	-7.281	0.000
Population	0.611	0.000	0.617	0.030
LST	0.186	0.151	0.126	0.669
LULC	-0.232	0.013	-0.512	0.016
Vegetation	-0.065	0.475	-0.095	0.648
Vehicle Population	14.000	0.001	22.000	0.005

The prediction model for $PM_{2.5}$ is:

$PM_{2.5}$=18.23 +1.12*households+1.57*Density of population-1.43*literacy rate+0.61 *Population -0.23 * LULC +14.00*Vehicle Population

The prediction model for PM_{10} is:

PM_{10}=55.47 +5.07*households + 3.91 *Density of population-7.28*literacy rate+0.61*Population -0.51* LULC+22.00*Vehicle Population

Conclusion

The study reveals that the particulate matter is below the standard value prescribed by the Central pollution control board. The highest air pollution in Chennai city is primarily responsible for vehicle population and industries. Wednesday and Thursday recorded maximum pollution in the study area, whereas Sunday was very low compared to other days. Regression shows that the vehicle populationis responsible for air pollution, followed by the population.Regression also reveals that vehicle population is highly responsible for PM_{10}, followed by $PM_{2.5}$.

Financial supports

The study has been funded by RUSA 2.0 "Research, Innovation and Quality Improvement" Data Analytics for Real-Time Monitoring and Prediction of Pollution in Chennai. Studies on Social and Behavioral Sciences and Linguistics (Theme-3).

Competing interests

The authors have declared no conflict of interest

Authors' contributions

Dr Yuvaraj R M: Conceptualization, Methodology,

Data curation, analysis, preparation of Map and Original draft preparation, M. Sakthivel and & M. R. Sindhumol: Data collection, Reviewing and Editing,

Acknowledgements

This study was carried out as part of the project funded by RUSA 2.0 "Research, Innovation and Quality Improvement" Data Analytics for Real-Time Monitoring and Prediction of Pollution in Chennai. Studies on Social and Behavioral Sciences and Linguistics (Theme - 3) in the Department of Geography, University of Madras. We thank the Central Pollution Control Board and State Pollution Control Board for providing the monitoring data.

Ethical considerations

Ethical issues (Including plagiarism, Informed Consent, misconduct, data fabrication and/or falsification, double publication and/or submission, redundancy, etc) have been completely ob-served by the authors).

References

1. Johnson TM, Guttikunda S, Wells GJ, Artaxo P, Bond TC, Russell AG, et al. Tools for improving air quality management: A review of top-down source apportionment techniques and their application in developing countries. Available from: http://hdl.handle.net/10986/17488

2. Goyal P, Krishna TR. Various methods of emission estimation of vehicular traffic in Delhi. Transportation Research Part D: Transport and Environment. 1998 Sep 1;3(5):309-17. Available from: http://dx.doi.org/10.1016/s1361-9209(98)00009-1

3. Cole MA, Neumayer E. Examining the impact of demographic factors on air pollution. Population and Environment. 2004 Sep 1:5-21. Available from: http://dx.doi.org/10.1023/b:poen.0000039950.85422.eb

4. Gore RW, Deshpande DS. An approach for classification of health risks based on air quality levels. In2017 1st International Conference on Intelligent Systems and Information Management (ICISIM) 2017 Oct 5 (pp. 58-61). IEEE. Available from: https://doi.org/10.1016/j.scitotenv.2021.148605

5. Litchfield I, Dockery D, Ayres J. Health effects of air pollution. Environmental Medicine [Internet]. 2010 Jul 30;141–52. Available from: http://dx.doi.org/10.1201/b13390-16

6. Shaddick G, Thomas ML, Mudu P, Ruggeri G, Gumy S. Half the world's population are exposed to increasing air pollution. NPJ Climate and Atmospheric Science. 2020 Jun 17;3(1):23. Available from: http://dx.doi.org/10.1038/s41612-020-0124-2

7. Ali MU, Liu G, Yousaf B, Ullah H, Abbas Q, Munir MA. A systematic review on global pollution status of particulate matter-associated potential toxic elements and health perspectives in urban environment. Environmental geochemistry and health. 2019 Jun 15;41:1131-62. Available from: http://dx.doi.org/10.1007/s10653-018-0203-z

8. Xu X, Xia J, Gao Y, Zheng W. Additional focus on particulate matter wash-off events from leaves is required: A review of studies of urban plants used to reduce airborne particulate matter pollution. Urban Forestry & Urban Greening. 2020 Feb 1;48:126559. Available from: http://dx.doi.org/10.1016/j.ufug.2019.126559

9. Diener A, Mudu P. How can vegetation protect us from air pollution? A critical review on green spaces' mitigation abilities for air-borne particles from a public health perspective-with implications for urban planning. Science of the Total Environment. 2021 Nov 20;796:148605.

10. Cole MA, Neumayer E. Examining the

impact of demographic factors on air pollution. Population and Environment. 2004 Sep 1:5-21. Available from: http://dx.doi.org/10.1023/b:poen.0000039950.85422.eb

11. Zou B, Peng F, Wan N, Mamady K, Wilson GJ. Spatial cluster detection of air pollution exposure inequities across the United States. PLoS One. 2014 Mar 19;9(3):e91917. Available from: http://dx.doi.org/10.1371/journal.pone.0091917.

12. Ilić I, Vuković M, Štrbac N, Urošević S. Applying GIS to Control Transportation Air Pollutants. Polish Journal of Environmental Studies. 2014 Sep 1;23(5). Available from: https://doi.org/10.18485/ecologica.2022.29.106.17

13. Syafei AD, Fujiwara A, Zhang J. A comparative study on NO concentration interpolation in Sena Baya city. Proceedings of the Eastern Asia Society for Transportation9. 2013:1-3. Available from: https://doi.org/10.1016/j.proenv.2015.07.061

14. Li L, Gong J, Zhou J. Spatial interpolation of fine particulate matter concentrations using the shortest wind-field path distance. PloS one. 2014 May 5;9(5):e96111. Available from: https://doi.org/10.1371/journal.pone.0096111.

15. Halek F, Kavousi-Rahim A. GIS assessment of the PM_{10}, $PM_{2.5}$ and PM1.0 concentrations in urban area of Tehran in warm and cold seasons. International Archives of the Photogrammetry, Remote Sensing & Spatial Information Sciences. 2014 Nov 15. Available from: http://dx.doi.org/10.5194/isprsarchives-xl-2-w3-141-2014

16. Barsi JA, Schott JR, Hook SJ, Raqueno NG, Markham BL, Radocinski RG. Landsat-8 thermal infrared sensor (TIRS) vicarious radiometric calibration. Remote Sensing. 2014 Nov 21;6(11):11607-26. Available from: http://dx.doi.org/10.3390/rs61111607.

17. J Jiménez-Muñoz JC, Sobrino JA, Gillespie A, Sabol D, Gustafson WT. Improved land surface emissivities over agricultural areas using ASTER NDVI. Remote Sensing of Environment. 2006 Aug 30;103(4):474-87. Available from: http://dx.doi.org/10.1016/j.rse.2006.04.012.

18. Carlson TN, Ripley DA. On the relation between NDVI, fractional vegetation cover, and leaf area index. Remote sensing of Environment. 1997 Dec 1;62(3):241-52. Available from: http://dx.doi.org/10.1016/s0034-4257(97)00104-1.

19. Sobrino JA, Jiménez-Muñoz JC, Paolini L. Land surface temperature retrieval from LANDSAT TM 5. Remote Sensing of environment. 2004 Apr 30;90(4):434-40. Available from: http://dx.doi.org/10.1016/j.rse.2004.02.003.

20. Weng Q, Lu D, Schubring J. Estimation of land surface temperature–vegetation abundance relationship for urban heat island studies. Remote sensing of Environment. 2004 Feb 29;89(4):467-83. Available from: http://dx.doi.org/10.1016/j.rse.2003.11.005.

21. Wang F, Qin Z, Song C, Tu L, Karnieli A, Zhao S. An improved mono-window algorithm for land surface temperature retrieval from Landsat 8 thermal infrared sensor data. Remote sensing. 2015 Apr 10;7(4):4268-89. Available from: http://dx.doi.org/10.3390/rs70404268.

22. Stathopoulou M, Cartalis C. Daytime urban heat islands from Landsat ETM+ and Corine land cover data: An application to major cities in Greece. Solar Energy. 2007 Mar 1;81(3):358-68. Available from: http://dx.doi.org/10.1016/j.solener.2006.06.014

23. Fredy Alejandro GL, Marco Andres GL, Nestor Yezid RR. Spatial-temporal assessment and mapping of the air quality and noise pollution in a sub-area local environment inside the center of a Latin American Megacity: Universidad Nacional de Colombia-Bogotá Campus. Asian Journal of Atmospheric Environment. 2018;12(3):232-43. Available from: http://dx.doi.org/10.5572/ajae.2018.12.3.232.

24. Zhang X, Gong Z. Spatiotemporal characteristics of urban air quality in China

and geographic detection of their determinants. Journal of Geographical Sciences. 2018 May;28:563-78. Available from: http://dx.doi.org/10.1007/s11442-018-1491-z

25. Chen P. Visualization of real-time monitoring datagraphic of urban environmental quality. Eurasip Journal on Image and Video Processing. 2019 Dec;2019(1):1-9. Available from: http://dx.doi.org/10.1186/s13640-019-0443-6.